JTTEE5 20:139–144
DOI: 10.1007/s11666-010-9578-9
1059-9630/$19.00 © ASM International

High Temperature Mechanical Behavior of UHTC Coatings for Thermal Protection of Re-Entry Vehicles

G. Pulci, M. Tului, J. Tirillò, F. Marra, S. Lionetti, and T. Valente

(Submitted May 5, 2010; in revised form September 16, 2010)

In this work, the high temperature mechanical properties of ultra high temperature ceramics (UHTC) coatings deposited by plasma spraying have been investigated; particularly the stress-strain relationship of ZrB_2-based thick films has been evaluated by means of 4-point bending tests up to 1500 °C in air. Results show that at each investigated temperature (500, 1000, and 1500 °C) modulus of rupture (MOR) values are higher than the ones obtained at room temperature (RT); moreover at 1500 °C the UHTC coatings exhibit a marked plastic behavior, maintaining a flexural strength 25% higher compared to RT tested samples. The coefficient of linear thermal expansion (CTE) has been evaluated up to 1500 °C: obtained data are of primary importance for substrate selection, interface design and to analyze the thermo-mechanical behavior of coating-substrate coupled system. Finally, SEM-EDS analyses have been carried out on as-sprayed and tested materials in order to understand the mechanisms of reinforcement activated by high temperature exposure and to identify the microstructural modifications induced by the combination of mechanical loads and temperature in an oxidizing environment.

Keywords high temperature mechanical properties, plasma spray, thermal protection systems, UHTC

1. Introduction

In recent years, the ultra high temperature ceramics (UHTC) have been extensively investigated as innovative thermal protection systems (TPS) for aerospace vehicles as well as for other applications where oxidation and/or erosion resistance at high temperature (up to 2000 °C) are required. These materials have melting temperatures above 3000 °C, retain their strength at temperatures above 1200 °C, exhibit good thermal shock resistance, and can be modified with additives such as SiC and/or $MoSi_2$ (Ref 1-3) to promote oxidation resistance.

The ''sharp'' configuration of the leading edges and of the nose of re-entry vehicles is considered as one of the most interesting solutions to increase aerodynamic efficiency and vehicle maneuverability (Ref 4, 5), and so to improve the safety of manned space flight and decrease the costs of the missions. However, the sharp design implies sensibly higher thermal loads applied to the materials with respect to the blunt configuration: the thermal and chemical stability of UHTC compounds makes them candidates for use in the extreme environments associated with atmospheric re-entry of sharp structures (2000 °C and above with monatomic O and N), but also makes them suitable to hypersonic flight (1400 °C and above in air), and rocket propulsion (3000 °C and above in reactive chemical vapors) (Ref 6).

The use of monolithic ceramics in large and hot structures, such as the wing leading edges or nose cap of hypersonic vehicles, is strongly limited by the intrinsic brittleness of these materials and by the difficulty in manufacturing (sintering and machining) large ceramic components (Ref 7).

A possible solution is the use of thick UHTC coatings to protect the surface from the oxidizing and erosive environment, deposited on tough and heat resistant substrates, to guarantee a good overall reliability of the hot structure. However, a complete and specific knowledge of mechanical properties of UHTC coatings at high temperature is essential to predict the behavior of the composite structures in real operating conditions, where they must withstand significant structural loads. Fundamental information is also required to optimize

This article is an invited paper selected from presentations at the 2010 International Thermal Spray Conference and has been expanded from the original presentation. It is simultaneously published in *Thermal Spray: Global Solutions for Future Applications, Proceedings of the 2010 International Thermal Spray Conference*, Singapore, May 3-5, 2010, Basil R. Marple, Arvind Agarwal, Margaret M. Hyland, Yuk-Chiu Lau, Chang-Jiu Li, Rogerio S. Lima, and Ghislain Montavon, Ed., ASM International, Materials Park, OH, 2011.

G. Pulci, J. Tirillò, F. Marra, and **T. Valente**, Rome University ''la Sapienza'', ICMA Dept., Rome, Italy and INSTM Reference Centre ''Laboratory on Engineering of Surface Treatments'', via Eudossiana, 18, 00184 Rome, Italy; **M. Tului** and **S. Lionetti**, Centro Sviluppo Materiali S.p.A, via di Castel Romano, 100, 00128 Rome, Italy. Contact e-mail: m.tului@c-s-m.it.

coating-substrate combinations and improve the quality of the interface.

The design of innovative TPS has become today a strategic objective for the development of re-usable launch vehicles (RLVs) endowed with high efficiency, maneuverability and reliability, and requiring at the same time lower costs and times for maintenance procedures after re-entry. It seems important to emphasize that significant further improvements in TPS reusability can only be expected by the identification of materials endowed with both increased high temperature oxidation resistance and mechanical properties, that is developing new compositions and innovative TPS architectures.

The experimental activities described in this article concern the high temperature mechanical characterization of ZrB_2-SiC (30% vol.)-$MoSi_2$ (10% vol.) plasma-sprayed coatings. This composition was selected because of its recognized excellent oxidation resistance at high temperatures (Ref 8, 9), proved even better than that of ZrB_2-SiC mixtures. However, no data is currently available about the mechanical properties at high temperature of UHTC coatings containing $MoSi_2$. The aim of this work was to carry out an extensive mechanical characterization of these coatings in the range room temperature (RT), 1500 °C.

2. Experimental

Powders were prepared by mixing and agglomerating by spray drying commercial powders (H.C. Starck) of ZrB_2 (60% vol.), SiC (30% vol.), and $MoSi_2$ (10% vol.); more details about agglomeration parameters can be found in (Ref 4).

Agglomerated particle size was examined by laser diffraction granulometry, whereas the phase composition was analyzed by means of x-ray diffraction technique. The powders were sprayed using a controlled atmosphere plasma spray (CAPS) apparatus (Sulzer Metco, CH), which allows atmosphere and pressure in the deposition chamber to be controlled during spraying. Coatings were deposited in inert gas (Ar, 1200 mbar), in the high pressure plasma spraying (HPPS) mode, using a F4MB torch and a plasma gas mixture of Ar (55 SLPM) and H_2 (13 SLPM).

ZrB_2-SiC-$MoSi_2$ coatings (hereafter called ZSM) were deposited on 150 × 150 mm graphite plates and, after spraying, mechanically removed from the substrates and machined by spark erosion to obtain parallelepiped-shaped specimens (45 × 4 × 3 mm) used for the thermo-mechanical characterization tests.

Mechanical behavior of ZSM was investigated by means of four-point bending tests performed at several temperatures (up to 1500 °C) and by the measure of the thermal expansion coefficient.

Four points bending tests were carried out at RT and at 500, 1000, 1500 °C in air by means of a Zwick-Roell Z2.5 testing machine equipped with a Maytec furnace (up to 1600 °C), a three-point-contact extensometer (able to auto-compensate for thermal strain) and a SiC flexure device, Fig. 1.

Fig. 1 The SiC flexure device and a tested (1500 °C) parallelepiped-shaped specimen

Testing parameters were selected according to ASTM C1211-02(2008): ''Standard Test Method for Flexural Strength of Advanced Ceramics at Elevated Temperatures.'' Bending tests were performed using a cross-head rate of 0.5 mm/min. The furnace, in which the sample is placed at RT, was heated at the rate of 10 °C/min, with a dwell time of 30 min at the testing temperature before the test start.

Ten samples were tested at RT, whereas at 500, 1000, and 1500 °C five tests were performed for each temperature. In this way, the stress-strain relationship at several temperatures in air was obtained and, particularly, the modulus of rupture (MOR), modulus of elasticity (MOE), and maximum bending strain of ZSM coatings were evaluated and compared.

SEM-EDS analyses were carried out on the cross section of specimens tested at different temperatures: the aim of these experimental activities was to determine microstructural modifications induced by simple mechanical load or by the synergistic effect of load and high temperature residence. More specifically, possible sintering effects and diffusion and oxidation phenomena caused by high temperature exposure were investigated, together with the crack formation and the damages induced by bending.

Finally, two ZSM samples (4 × 2 × 28 mm) were tested in a contact horizontal dilatometer (Linseis L76) in order to measure the coefficient of thermal expansion (CTE) parallel to the plane of coating from RT up to 1500 °C in air.

CTE measurement was performed according to ASTM E 228-06: ''Standard Test Method for linear Thermal Expansion of Solid Materials With a Push-Rod Dilatometer,'' with a heating rate of 3 °C/min.

Information on thermal expansion properties is of primary importance for the design of innovative TPS based on substrate-UHTC coating combinations. The development of reliable systems for high temperature applications is strictly connected to the minimization of stresses induced by coating-substrate CTE mismatch and to optimization of the interface, also using bond coats or graded deposition methods.

3. Results and Discussion

Figure 2 shows the results of laser granulometry on the agglomerated powder.

Powder granulometry exhibits a Gaussian-like distribution of particles, without evident asymmetrical tails or multi-modal trends and with a mean size of about 20 μm. The distribution shape highlights the effectiveness of the spray drying process: three different powders (ZrB_2, SiC, and $MoSi_2$) with different particle size appear as a monodispersed Gaussian distribution after the agglomeration treatment.

Figure 3 shows the result of XRD analysis performed on the spray dried powder; the x-ray diffraction pattern highlights the presence of ZrB_2, SiC and $MoSi_2$.

3.1 Four-Point Bending Tests

Results of mechanical tests are reported in the Table 1.

The stress-strain curves of four representative bending tests carried out on ZSM samples at different temperatures are reported and compared in Fig. 4.

The main mechanical properties obtained by bending tests at different temperatures can be compared.

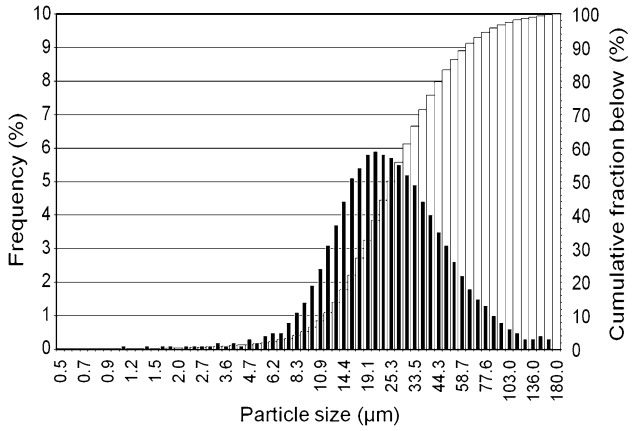

Fig. 2 Particle size distribution obtained by laser granulometry on agglomerated powder

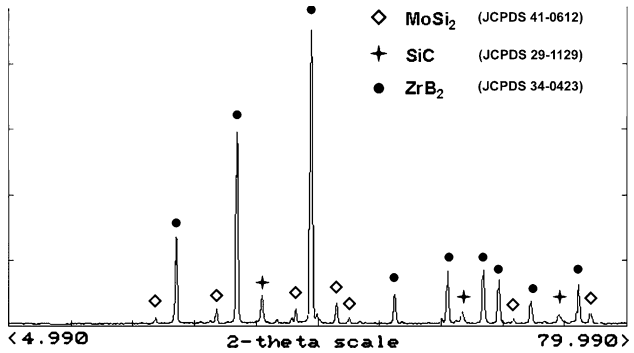

Fig. 3 XRD pattern of agglomerated powder

First of all, the data reveal that the MOR (i.e., flexural strength) increases as the test temperature rises to 1000 °C; at 1500 °C the mechanical response of the coatings totally changes: ZSM exhibits a MOR reduced by about 30% in comparison to results at 1000 °C. In the same way, the MOE increases at high temperatures but at 1500 °C decreases by about 60%.

Stress-strain curves at several temperatures (Fig. 4) highlight very well the variations in mechanical properties. Tested coatings show a brittle behavior, typical of ceramic materials, up to 1000 °C; at 1500 °C instead, ZSM exhibits a large plastic deformation above the load level of 50-70 MPa. At lower stress levels, ZSM maintains a relatively high stiffness: at 1500 °C the elastic modulus, evaluated between 10 and 50 MPa, is 84 GPa, lower by only 22% than the MOE at RT. Transition from brittle to plastic behavior between 1000 and 1500 °C is highlighted by the deformation of bent samples (see Fig. 1): because of plastic deformation, at 1500 °C the maximum strain reaches 1.5%, while at 1000 °C (without evident plastic phenomena) reaches hardly 0.1%. SEM-EDS analyses were performed on the microstructure of the tested specimens to better understand the temperature-induced modifications, Fig. 5 and 6.

The results of mechanical characterization seem to indicate the presence of at least two mechanisms acting at different temperatures and involving completely opposite effects: (i) an improvement of mechanical properties as

Table 1 Results of 4-point bending tests at different temperatures

	Modulus of elasticity, GPa		Modulus of rupture, MPa		Maximum strain, %	
Test temperature	Average	SD	Average	SD	Average	SD
Room temperature	108	6.3	115.1	6.5	0.12	0.02
500 °C	185	9.8	179.4	1.9	0.10	0.01
1000 °C	205	0.6	201.9	70.1	0.10	0.10
1500 °C	84	4.5	144.3	4.0	1.51	0.10

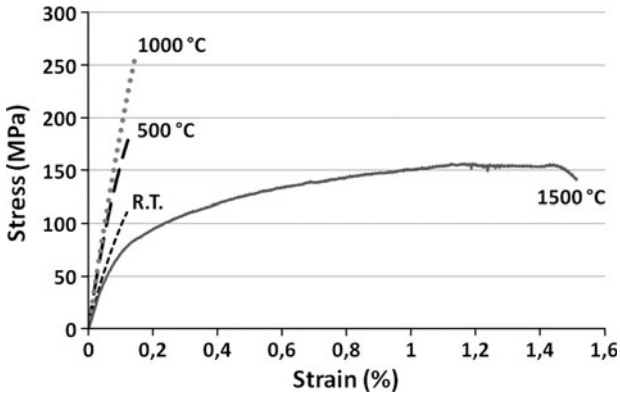

Fig. 4 Comparison of ZSM stress-strain relationship at several temperatures

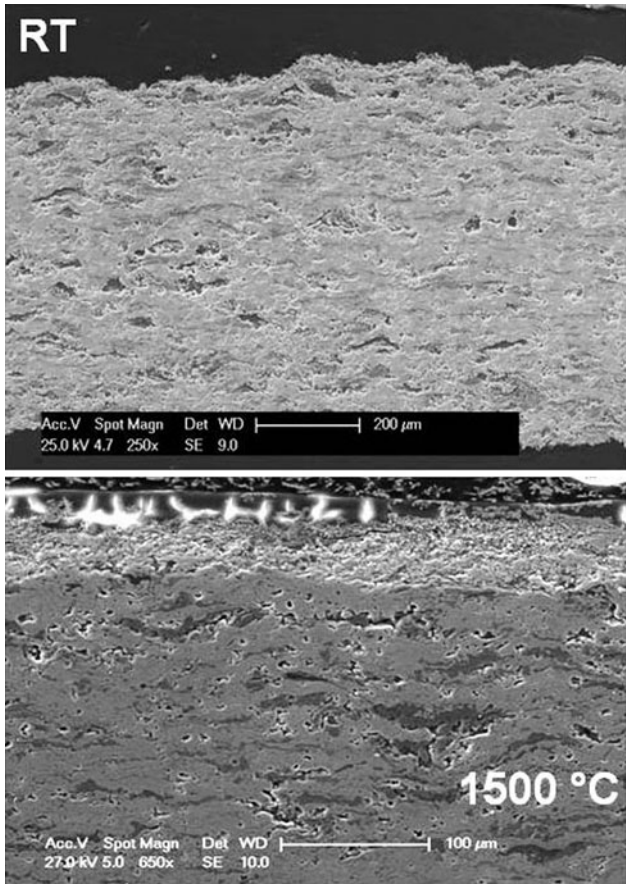

Fig. 5 SEM micrographies: samples (side in tension) after mechanical tests at RT (up) and 1500 °C (down)

the temperature increase up to 1000 °C and (ii) a completely changed behavior at 1500 °C, with a loss of stiffness and strength and the presence of an evident plastic deformation.

Moreover, other remarks can be made by observing the stress-strain curves: at RT, 500 and 1000 °C ZSM exhibits a nonlinear elastic behavior. In fact, though no permanent/plastic deformation was observed at these temperatures (elastic behavior), the constitutive relation is not linear: the tangent elastic modulus, evaluated as the slope of the stress-strain curve, decreases as the load rises. This is a well-known phenomenon typical of sprayed coatings and due to their loosely connected, open microstructure (Ref 10-13).

In Fig. 5, the microstructures of ZSM coatings tested at RT and at 1500 °C are shown; the first micrograph highlights the typical microstructure of an as-sprayed coating, made of splats, partially melted particles and pores (about 15% of porosity evaluated by image analysis). More specifically, in the as-sprayed plasma coating larger irregular pores could be found between the splats, small spherical pores inside the splats, imperfect bonding between the splats (intersplat cracks) and microcracks approximately perpendicular to the spraying plane formed during the rapid cooling (intrasplat cracks).

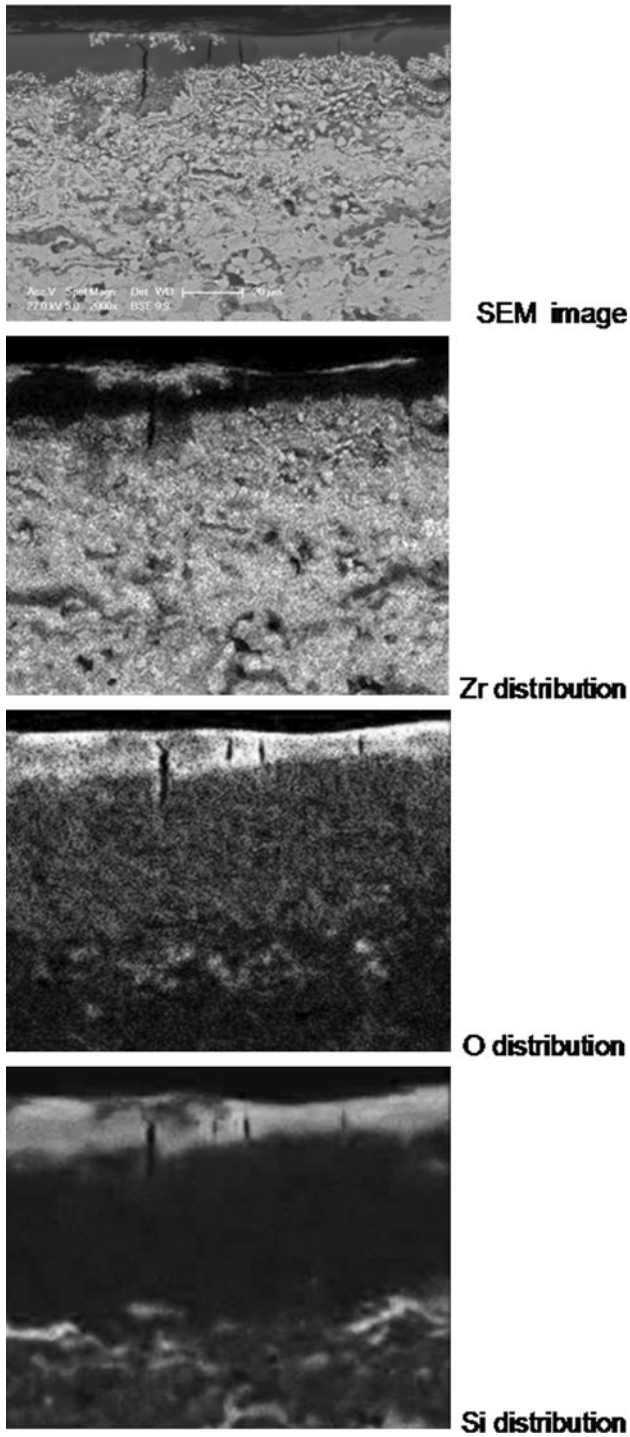

Fig. 6 SEM micrography of the oxide layer (side in tension) of a ZSM coating after bending test at 1500 °C; EDS maps show the elemental distribution

Although the intersplat and intrasplat cracks give only a small contribution to the total porosity, they are believed to be the main factor causing the stiffness decrease (Ref 14-17). The microstructure of a specimen tested at 1500 °C is shown in the second micrography of Fig. 5: the sample exhibits a denser microstructure, with a residual

porosity but a higher splat cohesion due to the sintering effect of the high temperature treatment. This is probably the reason of the relatively high value of MOE at 1500 °C: the stiffness reduction due to high temperature is partially compensated by the sintering effect (Ref 18). Micrography also shows the presence of a cracked oxide layer grown on the surface of the sample: a SEM-EDS analysis of the oxide scale (side in tension of specimen bent at 1500 °C) in order to better understand the layer composition and the element distribution is shown in Fig. 6.

The analysis highlights the presence of a silica scale on the surface with a ZrO_2 layer underneath, depleted of Si. This is in accordance with expected reactions, taking into account the high vapor pressure of boron and molybdenum oxide at temperatures greater than 1000 and 500 °C, respectively (Ref 19, 20):

$$ZrB_2 + 2.5\,O_2(g) \rightarrow ZrO_2 + B_2O_3(l)$$

$$SiC + 2O_2(g) \rightarrow SiO_2 + CO_2(g)$$

$$MoSi_2 + 3.5O_2(g) \rightarrow MoO_3 + 2SiO_2$$

SEM micrography also shows the formation of transversal cracks, presumably induced by the tensile stress state present on the surface of bent samples; it is very interesting to note that the cracks are not open, but are sealed toward the outside by thin scales rich in zirconium and oxygen. This sealing effect probably does not guarantee an effective protection from oxidation (ZrO_2 permits ionic diffusion of oxygen) but could avoid the presence of open cracks on the surface, improving in this way the mechanical properties at high temperature in oxidizing environments. In the same manner, the silica glass formation guarantees an healing effect for the surface defects (Ref 1). Sealing mechanisms of surface cracks are probably involved also at 1000 °C; previous works (Ref 9) showed the presence of a surface oxide scale in ZrB_2-$MoSi_2$ ceramics at temperatures above 700 °C: therefore the sintering and the healing of surface defects by oxide formation are probably the strengthening mechanisms active at 1000 °C.

The improvement in mechanical properties of samples tested at 500 °C cannot be explained considering sintering effects because of the too low temperature: in this case the main strengthening factor could be the formation of a ZrO_2-B_2O_3 scale on surface, in accordance with the reactions reported before.

Further investigations have to be carried out to completely understand the mechanisms involved in the low temperature strengthening and in the plastic deformation at 1500 °C; several hypotheses could be made for the plastic behavior: maybe the most promising is a possible sliding mechanism between splats and grains due to the softening of a silica nano-film present on the starting powders.

3.2 Thermal Expansion

The thermal expansion of ZSM coatings was measured between RT and 1500 °C; results (CTE and elongation as a function of temperature) are reported in Fig. 7.

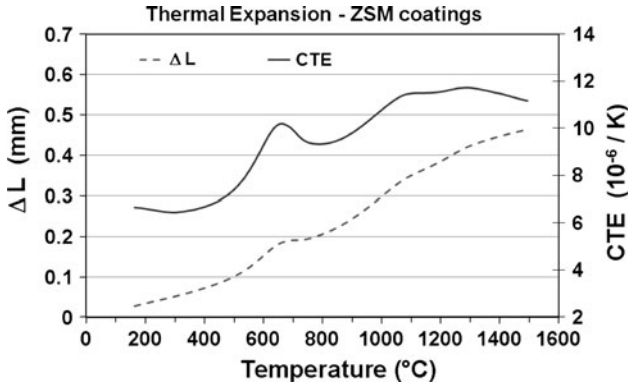

Fig. 7 Thermal expansion of ZSM coatings

CTE ranges between 6.2 and 11.7 × (10^{-6}/K); on the basis of CTE-temperature plot, several comments can be made. Data seem to indicate the presence of a phase transition and/or structural modifications between 500 and 800 °C; in this temperature range different phenomena coexist: (i) melting of B_2O_3, (ii) pesting of $MoSi_2$ (high rate evaporation of molybdenum oxide), and (iii) an inflexion point in the CTE diagram of SiC (Ref 7, 21). All these phenomena, especially if synergistic, could explain this particular trend between 500 and 800 °C.

Moreover, data highlight a particular behavior at high temperature: between 1100 and 1300 °C the curve shows a plateau and at higher temperature CTE decreases. This behavior can be related to sintering caused by high temperature exposure, as already shown in Fig. 5; the shrinkage, induced by sintering, partially compensates the elongation due to thermal expansion: the samples length falls from about 28.2 mm before the test to about 25.5 mm at RT at the end of test.

4. Conclusions

High temperature mechanical properties of ZrB_2-SiC (30% vol.)-$MoSi_2$ (10% vol.) plasma-sprayed coatings were investigated by means of four-point bending tests at different temperatures (up to 1500 °C) in air, and the CTE was evaluated by a contact horizontal dilatometer, also in this case up to 1500 °C in air.

Results shows an improvement in mechanical properties (MOR and MOE) as the temperature increase up to 1000 °C; at 1500 °C ZSM coatings maintain good mechanical properties but exhibit an evident plastic behavior; these results can be explained considering sintering and self-healing effects induced by the exposure at high temperature in an oxidizing environment.

References

1. D. Sciti, F. Monteverde, S. Guicciardi, G. Pezzotti, and A. Bellosi, Microstructure and Mechanical Properties of ZrB_2-$MoSi_2$ Ceramic Composites Produced by Different Sintering Techniques, *Mater. Sci. Eng. A*, 2006, **434**, p 303-309

2. J. Cook, A. Khan, E. Lee, and R. Mahapatra, Oxidation of $MoSi_2$-Based Composites, *Mater. Sci. Eng. A*, 1992, **155**(1-2), p 183-198
3. G. Reisel, B. Wielage, S. Steinhauser, I. Morgenthal, and R. Scholl, High Temperature Oxidation Behavior of HVOF-Sprayed Unreinforced and Reinforced Molybdenum Disilicide Powders, *Surf. Coat. Technol.*, 2001, **146-147**, p 19-26
4. C. Bartuli, T. Valente, and M. Tului, Plasma Spray Deposition and High Temperature Characterization of ZrB_2-SiC protective coatings, *Surf. Coat. Technol.*, 2002, **155**, p 260-273
5. T. Valente, C. Bartuli, and G. Pulci, Ceramic Composites and Thermal Protection Systems for Reusable Re-Entry Vehicles, *Adv. Sci. Technol.*, 2006, **45**, p 1505-1514
6. W.G. Fahrenholtz and G.E. Hilmas, NSF-AFOSR Joint Workshop on Future Ultra-High Temperature Materials, Workshop Report, Arlington, 2004
7. M.J. Gasch, D.T. Ellerby, and S.M. Johnson, Ultra High Temperature Ceramic Composites, *Handbook of Ceramic Composites*, N.P. Bansal, Ed., Kluwer Academic Publishers, Boston, 2005,
8. M. Tului, S. Lionetti, G. Marino, R. Gardi, T. Valente, and G. Pulci, *Thermal Spray 2009: Proceedings of the International Thermal Spray Conference*, p 634-638
9. D. Sciti, M. Brach, and A. Bellosi, Long-Term Oxidation Behavior and Mechanical Strength Degradation of a Pressureless Sintered ZrB_2-$MoSi_2$ Ceramic, *Scr. Mater.*, 2005, **53**, p 1297-1302
10. S.R. Choi, D. Zhu, and R.A. Miller, Deformation and Strength Behavior of Plasma-Sprayed ZrO_2-8 wt% Y_2O_3 Thermal Barrier Coatings in Biaxial Flexure and Trans-Thickness Tension, *Ceram. Eng. Sci. Proc.*, 2000, **21**(4), p 653-661
11. S.H. Leigh, C.K. Lin, and C.C. Berndt, Elastic Response of Thermal Spray Deposits Under Indentation Tests, *J. Am. Ceram. Soc.*, 1997, **80**(8), p 2093-2099
12. E.F. Rejda, D.F. Socie, and T. Itoh, Deformation Behavior of Plasma-Sprayed Thick Thermal Barrier Coatings, *Surf. Coat. Technol.*, 1999, **113**(3), p 218-226
13. V. Harok and K. Neufuss, Elastic and Inelastic Effects in Compression in Plasma-Sprayed Ceramic Coatings, *J. Therm. Spray Technol.*, 2001, **10**(1), p 126-132
14. F. Kroupa, Plesek Nonlinear Elastic Behavior in Compression of Thermally Sprayed Materials, *J. Mater. Sci. Eng. A*, 2002, **328**, p 1-7
15. J.I. Eldridge, G.N. Morscher, and S.R. Choi, Quasistatic vs. Dynamic Modulus Measurements of Plasma-Sprayed Thermal Barrier Coatings, *Ceram. Eng. Sci. Proc.*, 2002, **23**(4), p 371 ff
16. Y. Liu, T. Nakamura, V. Srinivasan, A. Vaidya, A. Gouldstone, and S. Sampath, Non-Linear Elastic Properties of Plasma-Sprayed Zirconia Coatings and Associated Relationships with Processing Conditions, *Acta Mater.*, 2007, **55**, p 4667-4678
17. T. Wakui, J. Malzbender, and R.W. Steinbrech, Strain Dependent Stiffness of Plasma Sprayed Thermal Barrier Coatings, *Surf. Coat. Technol.*, 2006, **200**, p 4995-5002
18. M. Tului, S. Lionetti, G. Pulci, E. Rocca, T. Valente, and G. Marino, Effects of Heat Treatments on Oxidation Resistance and Mechanical Properties of Ultra High Temperature Ceramic Coatings, *Surf. Coat. Technol.*, 2008, **202**, p 4394-4398
19. W.C. Tripp and H.C. Graham, Thermogravimetric Study of the Oxidation of ZrB_2 in the Temperature Range of 800° to 1500°C, *J. Electrochem. Soc.*, 1971, **118**, p 1195-1199
20. Y.T. Zhu, M. Stan, S.D. Conzone, and D.P. Butt, Thermal Oxidation Kinetics of $MoSi_2$-Based Powders, *J. Am. Ceram. Soc.*, 1999, **82**, p 2785-2790
21. E.V. Clougherty, K.E. Wilkes, and R.P. Tye, *Research and Development of Refractory Oxidation Resistant Diborides, Part II, Vol 5: Thermal, Physical, Electrical and Optical Properties*, AFML-TR-68-190, Wright-Patterson Air Force Base, 1969